motor, preceding the force generation, that produces a cut-off frequency above which power cannot effectively be injected into cochlear mechanics. □

Methods

Cell preparation. The isolation technique was similar to that described previously[12,13]. Adult guinea-pigs (200–400g) were killed by rapid cervical dislocation and both bullae were removed. The organ of Corti was dissected in a phosphate-buffered balanced salt solution containing (mM): 142, NaCl; 4, KCl; 1, $CaCl_2$; 1.5, $MgCl_2$; 8, Na_2HPO_4; 2, NaH_2PO_4 adjusted to pH 7.25. The osmolality of the solution was adjusted to 323–325 mosM using D-glucose. Cells were isolated by triturating the dissected tissue after incubation in 0.25 mg trypsin per ml (Sigma, type III) for 15 min. Extracellular solutions contained 142 NaCl, 4 KCl, 1.5 $MgCl_2$, 1 $CaCl_2$, 10 HEPES, adjusted to pH 7.3 with 1 M NaOH and to 325 mOsM using D-glucose. Pipette solutions for isolated patch experiments contained external solution with the addition of 10 mM $BaCl_2$ to block potassium channels. Conventional patch and whole-cell voltage-clamp recording techniques used an Axopatch 200 A amplifier (Axon, USA) to record from cells in a temperature-controlled chamber. Giga-seals were formed on the lateral walls of cells using low-resistance (1–4 MΩ) patch electrodes with the largest diameter possible (approximately 3 μm). Pipettes were coated with ski wax (Toko, Switzerland) or Sylgard to minimize capacitance. Patches were held at −20 mV to monitor the patch current, usually <1 pA. Data were filtered at 60 kHz and sampled at 333 kHz, unless stated. This sampling rate limited all time-resolved data to 3 μs. Standard P/4 methods were used to remove residual patch leak and linear capacitative currents[10] based on evidence from whole-cell recording that the motor charge movement takes place over a limited voltage range. Patches were stepped from the holding potential to the leak holding potential of −130 or +40 mV, and data were averaged as indicated. Data were fitted using a Levenberg–Marquardt algorithm based on 250 points. The standard error of the time constant estimate was less than 1.2 μs.

Capacitance. Patch capacitance was measured using a conventional lock-in amplifier (Stanford Research SR 530) and a patch amplifier (Axopatch 200 A). Sinusoidal commands (10 mV below 10 kHz and 0.5 mV above 10 kHz to avoid amplifier saturation) were summed with a command ramp (−80 to +130 mV) and fed directly to the head stage. Capacitance at each frequency was calibrated using a 100 fF dither circuit. The phasor angle was adjusted to measure only the absolute change in capacitance. Measurements between 1 and 90 kHz were made in a pseudo-random order. The frequency-dependent capacitance of the OHC patch, $C(f)$, is a sum of a voltage-independent linear term C_{patch} and a voltage-dependent term $C_v(f)$. The latter was identified by using a Levenberg–Marquardt fitting algorithm to identify the derivative of the Boltzmann curve (equation (1)) at each frequency.

Received 1 May; accepted 10 June 1997.

1. Davis, H. An active process in cochlear mechanics. *Hearing Res.* **9,** 79–90 (1983).
2. Dallos, P. in *The Cochlea* (eds Dallos, P., Popper, A. N. & Fay, R. R.) 1–43 (Springer, New York, 1996).
3. Mammano, F. & Nobili, R. Biophysics of the cochlea: linear approximation. *J. Acoust. Soc. Am.* **93,** 3320–3332 (1993).
4. Kalinec, F., Holley, M. C., Iwasa, K. H., Lim, D. J. & Kachar, B. A membrane-based force generation in auditory sensory cells. *Proc. Natl Acad. Sci. USA* **89,** 8671–8675 (1992).
5. Dallos, P. & Evans, B. High frequency motility of outer hair cells and the cochlear amplifier. *Science* **267,** 2006–2009 (1995).
6. Ashmore, J. F. Forward and reverse transduction in the mammalian cochlea. *Neurosci. Res.* **11** (suppl.), 39–50 (1990).
7. Santos-Sacchi, J. Reversible inhibition of voltage dependent outer hair cell motility and capacitance. *J. Neurosci.* **9,** 2954–2962 (1991).
8. Forge, A. Structural features of the lateral walls in mammalian cochlear outer hair cells. *Cell Tiss. Res.* **265,** 473–483 (1991).
9. Gale, J. E. & Ashmore, J. F. The outer hair cell motor in membrane patches. *Eur. J. Physiol.* **434,** 267–271 (1997).
10. Armstrong, C. M. & Bezanilla, F. Inactivation of the sodium channel. II Gating current experiments. *J. Gen. Physiol.* **70,** 567–590 (1977).
11. Iwasa, K. H. A membrane motor model for the fast motility of the outer hair cell. *J. Acoust. Soc. Am.* **96,** 2216–2224 (1994).
12. Tunstall, M. J., Gale, J. E. & Ashmore, J. F. Action of salicylate on membrane capacitance of outer hair cells from the guinea pig cochlea. *J. Physiol. (Lond.)* **485,** 739–752 (1995).
13. Ashmore, J. F. A fast motile response in guinea pig outer hair cells: the cellular basis of the cochlear amplifier. *J. Physiol. (Lond.)* **388,** 323–347 (1987).
14. Santos-Sacchi, J. On the frequency limit and phase of outer hair cell motility: the effects of membrane filter. *J. Neurosci.* **12,** 1906–1916 (1992).
15. Neher, E. & Marty, A. Discrete changes of cell membrane capacitance observed under conditions of enhanced secretion in bovine adrenal chromaffin cells. *Proc. Natl Acad. Sci. USA* **79,** 6712–6716 (1982).
16. Maconochie, D. J., Fletcher, G. H. & Steinbach, J. H. The conductance of the muscle nicotinic receptor channel changes rapidly upon gating. *Biophys. J.* **68,** 483–490 (1995).
17. Sigg, D., Stefani, E. & Bezanilla, F. Gating current noise produced by elementary transitions in Shaker potassium channels. *Science* **264,** 578–582 (1994).
18. Conti, F. & Stühmer, W. Quantal charge redistributions accompanying the structural transitions of sodium channels. *Eur. Biophys. J.* **17,** 53–59 (1989).
19. Hilgemann, D. W. Channel-like function of the Na, K pump probed at microsecond resolution in giant membrane patches. *Science* **263,** 1429–1432 (1994).
20. Gadsby, D. C., Rakowski, R. F. & De Weer, P. Extracellular access to the Na,K pump: pathway similar to ion channel. *Science* **260,** 100–103 (1993).
21. Rakowski, R. F. Charge movement by the Na,K pump in *Xenopus* oocytes. *J. Gen. Physiol.* **101,** 117–144 (1993).
22. Yang, N. B., George, A. L. Jr & Horn, R. Molecular basis of charge movement in voltage gated sodium channels. *Neuron* **15,** 213–218 (1995).
23. Ashmore, J. F. & Holley, M. C. Temperature dependence of a fast motile response in isolated outer hair cells of the guinea-pig cochlea. *Q. J. Exp. Physiol.* **73,** 143–145 (1988).
24. Vater, M. & Lenoir, M. Ultrastructure of the Horseshoe bat's organ of Corti. I. Scanning electron microscopy. *J. Comp. Neurol.* **318,** 367–379 (1992).

Acknowledgements. This work was supported by the Hearing Research Trust, the Colt Foundation, the Royal Society, and the Wellcome Trust.

Correspondence and requests for materials should be addressed to J.F.A. (e-mail: j-ashmore@ucl.ac.uk).

Modulation of neuronal activity by target uncertainty

Michele A. Basso & Robert H. Wurtz

Laboratory of Sensorimotor Research, National Eye Institute, Bethesda, Maryland 20892-4435, USA

Visual scenes are composed of many elements and although we can appreciate a scene as a whole, we can only move our eyes to one element of the scene at a time. As visual scenes become more complex, the number of potential targets in the scene increases, and the uncertainty that any particular one will be selected for an eye movement also increases. How motor systems accommodate this target uncertainty remains unknown. The activities of neurons in both the cerebral cortex[1–5] and superior colliculus[6–8] are modulated by this selection process. We reasoned that activity associated with target uncertainty should be evident in the saccadic motor system at the final stages of neural processing, in the superior colliculus[9,10]. By systematically changing the number of stimuli from which a selection must be made and recording from superior colliculus neurons, we found that as the target uncertainty increased, the neural activity preceding target selection decreased. These results indicate that neurons within the final common pathway for movement generation are active well in advance of the selection of a particular movement. This early activity varies with the probability that a particular movement will be selected.

The intermediate layers of the superior colliculus receive input from extensive regions of the cerebral cortex and may be regarded as a virtual readout of the cerebral cortex for the control of eye movements. Moreover, prelude burst neurons and buildup neurons in the superior colliculus increase their activity with the selection and preparation of a movement long before the activity closely related to saccade generation[6–8]. We determined the effect of target uncertainty on buildup neurons in awake monkeys in two ways. In the first experiment, we manipulated target uncertainty by presenting a different number of possible targets to monkeys on different trials. In a second experiment, we manipulated target uncertainty by presenting the same visual array of possible targets on every trial and varying the probability that any one of the stimuli would be selected for a saccadic eye movement. In both experiments we found that buildup neurons decreased their activity as uncertainty increased.

One, two, four or eight possible targets were introduced to increase uncertainty (Fig. 1: array on, uncertainty period), and then later the monkeys were cued as to which target was relevant (target dim, selection period). With a single possible saccadic target (Fig. 2, top row), neurons showed a transient visual response (left

spike density function) a subsequent sustained response which continued after the target dimmed (centre column), and then a burst of activity before the saccade to that target (right column).

During the period of uncertainty, increasing the number of possible targets in the array from one to two, to four and then to eight (Fig. 2) reduced the initial visual response. The increasing number of possible targets also decreased the activity after this initial visual response. At the end of the uncertainty period (before the dimming) the reduction continued as emphasized by the bold outline traces in the middle column of Fig. 2.

When the target dimmed, the uncertainty dropped to zero. In the single possible target case (Fig. 2, top row, middle column) there was no target uncertainty, the firing rate was already high and did not increase much further. With eight possible targets (bottom row, middle histogram), when there was maximal uncertainty in this task, the firing rate increased when the target was selected.

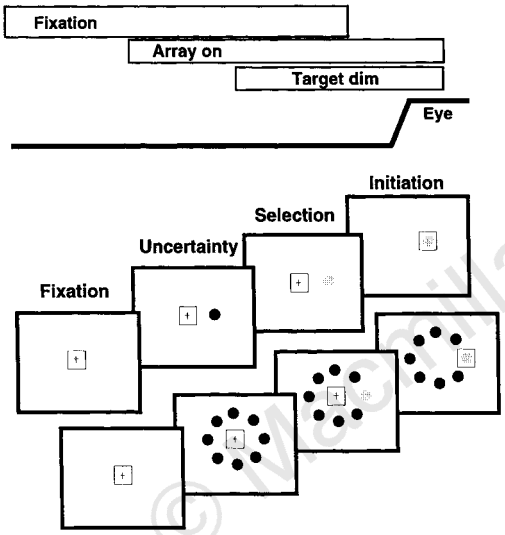

Figure 1 Behavioural task used for separating target uncertainty from target selection. Across the top of the figure a schematic of the temporal arrangement of the task is shown by the labelled time lines and the schematic eye position during the trials is also indicated (Eye). Below is the spatial arrangement of the stimuli on the tangent screen. Only the one possible target and eight possible target trial types are shown. The fixation point is shown as a cross and the stimulus spots are shown as black filled circles. The selected target is indicated schematically by the grey filled circle. The required eye position is indicated by a small square around the fixation point or the selected target.

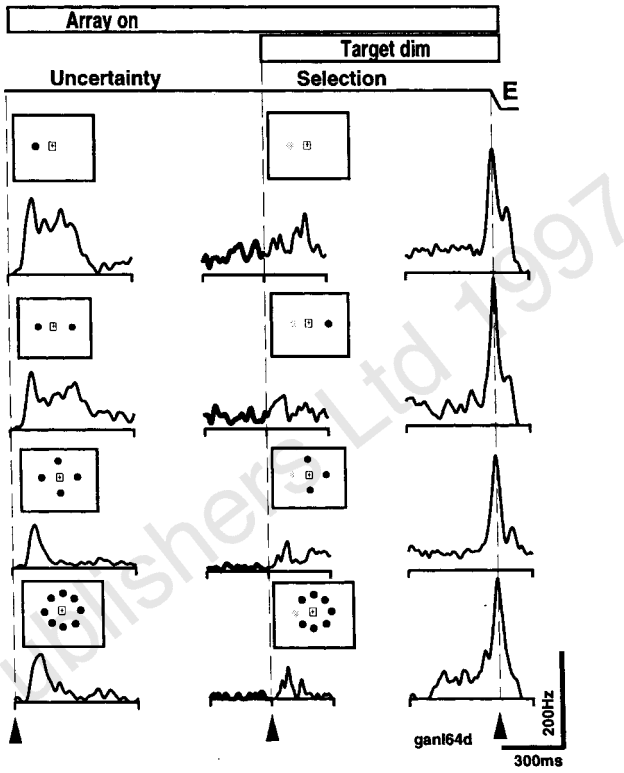

Figure 2 Decreased neuronal activity with increased uncertainty. The activity of a typical buildup neuron studied in the monkey superior colliculus during the three periods of the task is shown by spike density functions averaged over at least 6 trials. The schematic diagrams of the stimulus presentations indicate the trials with one, two, four or eight possible targets. In each column the alignment is indicated by the dashed vertical line and arrowhead. The left column, aligned on array onset, shows the phasic visual on-response and the following lower level of sustained discharge typical of all the neurons studied. The second column shows the shift from uncertainty to selection, and is aligned on target dimming. As the number of possible targets increases, the activity in the period of uncertainty decreases for both the visual on-response and the later sustained response (bold outline) of the buildup neurons. The third column is aligned on saccade initiation; the response amplitude was the same for all trial types. The saccade target was in the centre of the visual field where the burst of the neuron before the saccade was the strongest. The larger visual response with only one possible target (top row, left column) may reflect an enhancement in these saccade-related neurons reminiscent of such enhancement reported for the collicular visual neurons[16]. This enhancement would be most prominent with only one possible target because only in this case can the selection (and the accompanying enhancement) be made as soon as the stimulus appears. E is a schematic of eye position.

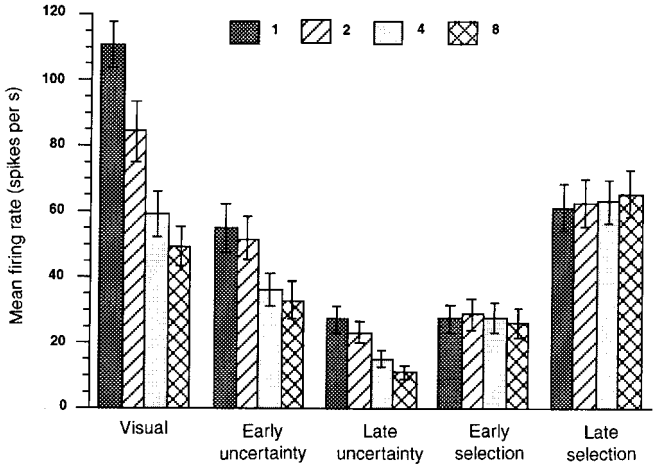

Figure 3 All neurons showed decreased activity with increased uncertainty. The graph shows the mean activity of 40 neurons from 2 monkeys with one to eight possible targets in the successive periods of the task. Activity decreased as the number of possible targets increased in the visual period (the first 150 ms after the minimal visual latency of intermediate layer SC neurons of 50 ms), in the early period of uncertainty following this visual response (the next 150 ms), and during a period of late uncertainty (200 ms before the target dimmed). In contrast, little change of activity was evident at early target selection (200 ms after the target dimmed) or late target selection (100 ms before the fixation point offset). Bars are 1 standard error of the mean. Note that although some individual neurons showed changes during the selection period (Fig. 2), this was not consistently observed across the sample of neurons (this figure).

All neurons in our sample showed decreasing firing rates during the period of uncertainty as the number of possible targets increased (Fig. 3). The activity decrease from one to eight possible targets was seen in the initial visual period (ANOVA $F(3,156) = 11.81$, $P < 0.001$), the early uncertainty (ANOVA $F(3,156) = 3.43$, $P < 0.02$), and the late uncertainty period (ANOVA $F(3,156) = 5.69$, $P < 0.001$). This difference was not evident during the selection period (early selection (ANOVA $F(3,156) = 0.06$, $P < 0.98$)) or just before the go signal (late selection (ANOVA $F(3,156) = 0.034$, $P < 0.99$)). Thus, the mean response of all 40 neurons in our sample decreased in the period from visual onset to target selection as target uncertainty increased. We also compared the difference between the responses in the one-target and eight-target conditions on a neuron by neuron basis using a Wilcoxon signed rank test. The differences for the intervals before the target selection were also significant on this test (visual, $P < 0.001$; early uncertainty, $P < 0.001$; late uncertainty, $P < 0.001$; early selection, $P < 0.46$; late selection, $P < 0.71$).

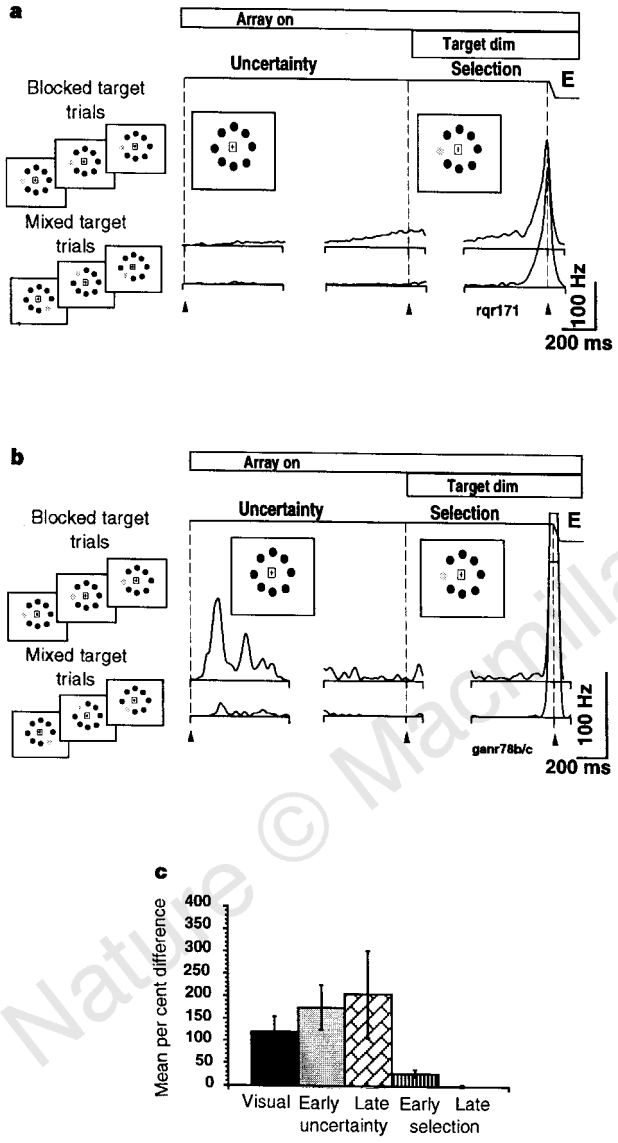

Figure 4 Uncertainty effects persist with individual visual stimuli. **a**, Comparison of the response of a single neuron for trials in which the target selected was always the same one of the eight possible targets (blocked trials) or varied among the eight possible targets (mixed target trials). Each spike density function is an average of 30 trials. The alignment is the same as in Fig. 3. In this task, the selected target and the fixation point offset occurred simultaneously. The neuron in this example had very little visual activity in the eight-target condition. **b**, Same as in **a** except this neuron had a more prominent visual response. Each spike density function is an average of 50 trials. **c**, Mean per cent difference (mean response blocked – mean response mixed/mean response mixed × 100) in activity of 32 neurons from two monkeys in the blocked and mixed target trials. Bars are 1 standard error of the mean. The intervals over which we quantified were the same as in Fig. 3. Because the target dimming and the fixation point turning off occurred simultaneously in this task the two periods of selection largely overlap. Note also that the differences in the neural activity during the different phases of uncertainty were variable across our sample of neurons (compare **a** and **b**), resulting in a large range of difference values . E is a schematic of eye position.

In a second experiment, we manipulated the level of target uncertainty by changing the monkey's previous experience on the task. We presented the same eight-stimulus array in two different conditions. In the mixed target condition, any one of the eight possible targets could be selected on any given trial, as in the first experiment. In the blocked trial condition, the same stimulus became the target on every trial. This task had the advantage that in both conditions the stimulus array was identical. Therefore any changes in the activity of neurons could not be attributed to changes in the visual display, but rather to changes in the level of uncertainty the monkeys had about the impending saccadic target. When the target in the response field of the neuron was presented as a saccadic goal repeatedly (blocked target trials) the uncertainty (based on the preceding trials) was minimized and the neuron had a high level of activity (Fig. 4a, top trace and b, top trace). In contrast, when uncertainty was high (mixed target trials) the activity of the neuron diminished (Fig. 4a, bottom trace and b, bottom trace). Quantifying the difference in activity in the blocked and mixed conditions again, using a paired neuron by neuron comparison (Fig. 4c), demonstrated that the modulation of activity in all uncertainty periods was statistically significant (Wilcoxon signed rank test; visual, $P < 0.001$; early uncertainty, $P < 0.001$; late uncertainty, $P < 0.001$) as was the activity during early selection ($P < 0.01$) whereas activity during late selection was not ($P < 0.30$).

Interestingly, the increase in neural activity that occurred in the blocked condition developed over time. For example, after the monkey was switched from mixed to blocked trials, the mean response during the late uncertainty period of the first 10 trials for the neuron depicted in Fig. 4a was 55.05 (s.e.m., 1.57) spikes per s. The mean response increased so that during this interval for the last 10 trials it was 89.65 (s.e.m., 15.70) spikes per s. Across our sample of 32 neurons, the difference in activity during the late uncertainty interval in the first and last 10 trials was statistically significant (Wilcoxon signed rank test, $P < 0.01$).

These experiments show that the activity of many saccade-related superior colliculus neurons changes substantially as the uncertainty of the target changes. Moreover, changes in target uncertainty modulate neuronal activity whether the uncertainty results from changes in the number of possible visual targets or changes in the monkeys' previous experience of which visual stimulus will become the selected target. Thus the buildup of activity that has been used to characterize these neurons[7] is dependent upon the conditions under which they are being studied. Moreover, the modulation of the vigour of sustained discharge in collicular neurons according to the degree of uncertainty raises the possibility that the change of uncertainty might also influence the activity of neurons in the cerebral cortex that are known to project to the superior colliculus. For example, neurons in the frontal cortex already have been found to alter their activity in the presence of multiple stimuli[3]. The change in neuronal activity with stimulus selection in other cortical areas not specifically related to the generation of movement, such as those studied in visual attention tasks, might also be altered more or less with changes of uncertainty in the tasks[11,12], as seems likely in area V4[13]. Finally, the possibility remains that the activity seen in the superior colliculus before the target selection may represent a

preliminary selection that is then either enhanced or suppressed by descending cortical influences. □

Methods

In two monkeys, we used standard electrophysiological techniques to record single neurons from the superior colliculus, monitor eye movements, and construct spike density histograms as described previously[7]. All experimental protocols were approved by the Institute of Animal Care and Use Committee and complied with Public Health Service policy on the humane care and use of laboratory animals. In all the trials, the monkey followed three steps. First, a central fixation point (projected light-emitting diode spot) came on in the centre of the screen, and the monkey was required to look at it to initiate the trial. Second, the array of possible targets came on. This was the period of uncertainty because which of the spots will become the target was not yet known to the monkeys. One, two, four or eight spots of light were generated by a TV projector, and these trial types were randomly interleaved. One of these spots was always located at the position in the field that yielded the maximal saccade-related activity of the neuron. All other targets were placed equally eccentric but in different directions (in the four cardinal and four oblique directions). Third, one of the spots dimmed. This was the period of selection because at this time the monkeys knew which of the spots was the target for the saccade. The removal of the fixation point served as a 'go' signal and the monkeys were then allowed to make a saccade (initiation). A liquid reward was given if the monkeys maintained their eye position at the target for 300 ms. The selection task was kept simple with a clear target change so that it was essentially a 'popout' task[14] requiring only target detection, not discrimination[15].

In the first experiment (Figs 1–3) the durations of successive periods were randomized among 800–1,200 ms to avoid timing behaviour by the monkey. The periods shown in Fig. 2 are 600 ms so there is no temporal overlap between the successive traces. Because we see the prominent effect of uncertainty in all of these neurons long before saccade onset, it makes little difference whether any given neuron is classified as a prelude burster or a buildup neuron, whether these neuronal categories largely overlap. In the second experiment (Fig. 4) only the probability that the target will be in the movement field of the neuron changes: 100% in blocked trials; 12.5% in mixed target trials. The level of uncertainty is determined by the monkey's experience in previous trials of a consistently located target or a randomly located target.

Received 30 January; accepted 17 June 1997.

1. Maunsell, J. H. R. The brain's visual world: representation of visual targets in cerebral cortex. *Science* **270,** 764–769 (1995).
2. Schall, J. D. & Hanes, D. P. Neural basis of saccade target selection in frontal eye field during visual search. *Nature* **366,** 467–469 (1993).
3. Schall, J. D., Hanes, D. P., Thompson, K. G. & King, D. J. Saccade target selection in frontal eye field of macaque. I. Visual and premovement activation. *J. Neurosci.* **15,** 6905–6918 (1995).
4. Kusunoki, M. & Goldberg, M. E. Responses of parietal visual neurons to attentionally significant stable objects. *Soc. Neurosci. Abstr.* **21,** 665 (1995).
5. Shadlen, M. N. & Newsome, W. T. Motion perception: Seeing and deciding. *Proc. Natl Acad. Sci. USA* **93,** 628–633 (1996).
6. Glimcher, P. W. & Sparks, D. L. Movement selection in advance of action in the superior colliculus. *Nature* **355,** 542–545 (1992).
7. Munoz, D. P. & Wurtz, R. H. Saccade-related activity in monkey superior colliculus. I. Characteristics of burst and buildup cells. *J. Neurophysiol.* **73,** 2313–2333 (1995).
8. Kustov, A. A. & Robinson, D. L. Shared neural control of attentional shifts and eye movements. *Nature* **384,** 74–77 (1996).
9. Sparks, D. L. & Hartwich-Young, R. in *The Neurobiology of Saccadic Eye Movements, Reviews of Oculomotor Research*, Vol. III (eds Wurtz, R. H. & Goldberg, M. E.) 213–256 (Elsevier, Amsterdam, 1989).
10. Miyashita, N. & Hikosaka, O. Minimal synaptic delay in the saccadic output pathway of the superior colliculus studied in awake monkey. *Exp. Brain Res.* **112,** 187–196 (1996).
11. Moran, J. & Desimone, R. Selective attention gates visual processing in extrastriate cortex. *Science* **229,** 782–784 (1985).
12. Treue, S. & Maunsell, J. H. Attentional modulation of visual motion processing in cortical areas MT and MST. *Nature* **382,** 539–541 (1996).
13. Motter, B. C. Focal attention produces spatially selective processing in visual cortical areas V1, V2, and V4 in the presence of competing stimuli. *J. Neurophysiol.* **70,** 909–919 (1993).
14. Treisman, A. M. & Gelade, G. A feature-integration theory of attention. *Cogn. Psych.* **12,** 97–136 (1980).
15. Bravo, M. J. & Makayama, K. The role of attention in different visual-search tasks. *Percept. Psychophys.* **51,** 465–472 (1992).
16. Goldberg, M. E. & Wurtz, R. H. Activity of superior colliculus in behaving monkeys. II. Effect of attention on neuronal responses. *J. Neurophysiol.* **35,** 560–574 (1972).

Acknowledgements. We thank the Laboratory of Diagnostic Radiology Research for magnetic resonance images. We thank J. Steinberg for secretarial assistance preparing the manuscript. We gratefully acknowledge the critical comments made on previous versions by J. Gottlieb and M. A. Sommer.

Correspondence and requests for materials should be addressed to M.A.B. (e-mail: mab@lsr.nei.nih.gov).

PrP-expressing tissue required for transfer of scrapie infectivity from spleen to brain

Thomas Blättler*, Sebastian Brandner*, Alex J. Raeber†, Michael A. Klein*, Till Voigtländer*, Charles Weissmann† & Adriano Aguzzi*

* *Institute of Neuropathology, Department of Pathology, University of Zürich, Schmelzbergstrasse 12, CH-8091 Zürich, Switzerland*
† *Institute of Molecular Biology, University of Zürich, Hönggerberg, CH-8093 Zürich, Switzerland*

Much available evidence points to a pathological isoform of the prion protein PrP being the infectious agent that causes transmissible spongiform encephalopathies, but the mechanisms controlling the neurotropism of prions are still unclear. We have previously shown that mice that do not express PrP (*Prnp*$^{o/o}$ mice) are resistant to infection by prions[1,2], and that if a *Prnp*$^{+/+}$ neurograft is introduced into such animals and these are infected intracerebrally with scrapie, the graft but not the surrounding tissue shows scrapie pathology[3]. Here we show that PrP-expressing neurografts in *Prnp*$^{o/o}$ mice do not develop scrapie histopathology after intraperitoneal or intravenous inoculation with scrapie prions. Prion titres were undetectable in spleens of inoculated *Prnp*$^{o/o}$ mice, but were restored to wild-type levels upon reconstitution of the host lymphohaemopoietic system with PrP-expressing cells. Surprisingly, however, i.p. or i.v. inoculation failed to produce scrapie pathology in the neurografts of 27 out of 28 reconstituted animals, in contrast to intracerebral inoculation. We conclude that transfer of infectivity from the spleen to the central nervous system is crucially dependent on the expression of PrP in a tissue compartment that cannot be reconstituted by bone marrow transfer. Thus the requirement for the normal isoform of PrP in peripheral tissues represents a bottleneck for the spread of prions from peripheral sites to the central nervous system.

We placed neurografts derived from wild-type mice or transgenic mice overexpressing PrP (*tga20*; ref. 4) into the brains of *Prnp*$^{o/o}$ mice and delivered scrapie prions (6.5 log LD_{50} units, where LD_{50} is the half-maximal lethal dose) by intraperitoneal (i.p.) or intravenous (i.v.) injection. Neither clinical disease nor the histopathological changes characteristic of spongiform encephalopathy developed during the observation period, up to 401 days after inoculation. Histoblots[5] revealed no protease-resistant PrP^{Sc} in *Prnp*$^{o/o}$ mice carrying *tga20* ($n = 17$) or wild-type ($n = 2$) neurografts. In contrast, the same amount of infectious agent produced scrapie when administered i.p. to 3/3 wild-type mice (incubation time, 209 ± 0 days) or 5/5 *tga20* mice (incubation time, 85 ± 2 days) (Table 1).

These results indicate that the spread of prions from the periphery to the brain of neurografted *Prnp*$^{o/o}$ mice is severely impaired, if not abolished. Three non-exclusive explanations can be offered: (1) prions administered peripherally must first replicate in peripheral organs, from where they invade the central nervous system (CNS); (2) prion spread is possible in the absence of peripheral PrP^{C}, but does not occur in *Prnp*$^{o/o}$ mice owing to the humoral immune response to PrP that occurs in such animals[6]; (3) whether they replicate or not, prions need a continuous chain of PrP^{C}-expressing tissues for centripetal propagation within the host.

Possibility (1) predicates that prions administered i.p. must undergo some replication in extracerebral compartments (a process that is impaired in *Prnp*$^{o/o}$ mice[7]) in order to reach the brain. In wild-type mice, the only tissue outside the CNS in which scrapie